Portability of Epimerization Domain and Role of Peptidyl Carrier Protein on Epimerization Activity in Nonribosomal Peptide Synthetases[†]

Uwe Linne, Sascha Doekel,[#] and Mohamed A. Marahiel*

Philipps Universität Marburg, Fachbereich Chemie/Biochemie, Hans-Meerwein-Strasse, 35032 Marburg, Germany

Received August 1, 2001; Revised Manuscript Received October 17, 2001

ABSTRACT: Incorporation of nonproteinogenic amino acids in small polypeptides synthesized by nonribosomal peptide synthetases (NRPS) significantly contributes to their biological activity. In these peptides, conversion of L-amino acids to the corresponding D-isomer is catalyzed by specialized NRPS modules that utilize an epimerization (E) domain. To understand the basis for the specific interaction of E domains with PCP domains (peptidyl carrier proteins, also described as T domains) and to investigate their substrate tolerance, we constructed a set of eight fusion proteins. The gene fragments encoding E and PCP-E domains of TycA (A-PCP-E), the one module tyrocidine synthetase A, were fused to different gene fragments encoding A and A-PCP domains, resulting in A/PCP-E and A-PCP/E types of fusion proteins (slash indicates site of fusion). We were able to show that the E domain of TycA, usually epimerizing Phe, does also accept the alternate substrates Trp, Ile, and Val, although with reduced efficiency. Interestingly, however, an epimerization activity was only observed in the case of fusion proteins where the PCP domain originates from modules containing an E domain. Sequence comparison revealed that such PCPs possess significant differences in the signature Ppant binding motif (CoreT: [GGDSI]), when compared to those carrier proteins, originating from ordinary C-A-PCP elongation modules (CoreT: [GGHSL]). By means of mutational analysis, we could show that epimerization activity is influenced by the nature of amino acid residues in proximity to the cofactor Ppant binding site. The aspartate residue in front of the invariant serine (Ppant binding site) especially seems to play an important role for the proper interaction between PCP and the E domain, as well as the presentation of the aminoacyl-S-Ppant substrate in the course of substrate epimerization. In conclusion, specialized PCP domains are needed for a productive interaction with E domains when constructing hybrid enzymes.

In bacteria and fungi, the biosynthesis of many polypeptides of pharmacological interest is carried out by nonribosomal peptide synthetases (NRPS[1]) (*1*−*3*). These large multifunctional enzymes possess a modular organization and provide an alternative itinerary to ribosomal peptide synthesis (*4*, *5*). NRPS products show several specific structural features, including cyclization and the incorporation of nonproteinogenic amino acids, especially D-isomers (*6*). The building blocks of NRPS, the modules, can be subdivided into domains, each responsible for one catalytic function (*7*). For example, the adenylation domain (A domain) is responsible for substrate recognition and activation as aminoacyl-O-AMP by hydrolysis of ATP (*8*). The peptidyl carrier protein (PCP domain, also described as thiolation (T) domain) is known to bind the activated amino acids or the growing peptide intermediates as thioester to the cofactor 4′-phosphopantetheine (Ppant) (*9*, *10*). This cofactor is covalently tethered to an invariant serine residue within a highly conserved region of the PCP domain, the so-called CoreT (GG[H,D]S[L,I]) (*4*, *7*). Posttranslational modification of the PCP domains in each module is catalyzed by a special class of CoASH-binding 4′-phosphopantetheinyl transferases (*11*, *12*). In addition to the A and the PCP domains, representing the basic equipment of an initiation module, elongation modules contain an additional condensation domain (C domain) that catalyzes the formation of a peptide bond between the nascent peptidyl-S-Ppant and the attacking aminoacyl-S-Ppant nucleophile (*13*). Furthermore, the C domain was described to harbor two selective substrate-binding sites (*14*): an enantioselective electrophilic donor site

[†] This work has been supported by the Deutsche Forschungsgemeinschaft and the Fonds der chemischen Industrie.

* To whom correspondence should be addressed. Tel: ++49-6421-2825722. Fax: ++49-6421-2822191. E-mail: marahiel@chemie.uni-marburg.de.

[#] Present address: Cubist Pharmaceuticals Inc., 300-2386 East Mall Road UBC, Vancouver, Canada.

[1] Abbreviations: A, adenylation domain; aminoacyl or peptidyl-S-Ppant, aminoacylated thioester form of cofactor Ppant bound to the strictly conserved serine residue of PCPs; ATP, adenosine 5′-triphosphate; C, condensation domain; CoASH, coenzyme A; DKP, D,L-diketopiperazine; DTE, 1,4-dithioerythritol; E, epimerization domain; EDTA, ethylendiamintetraacetic acid; HPLC, high-performance liquid chromatography; LSC, liquid scintillation counting; NRPS, nonribosomal peptide synthetase; PCR, polymerase chain reaction; PCP, peptidyl carrier protein, referring to the same thing as "T", but used in the text to stress the function of the protein (in analogy to the well-known ACPs of fatty acid synthases and polyketide synthases); PCP^{C}, PCP normally localized in front of a C domain; PCP^{E}, PCP naturally connected to an E domain; Ppant, 4′-phosphopantetheine; PP_i, inorganic pyrophosphate; T, thiolation domain, referring to the same thing as "PCP", but used for the description of proteins ("one letter−one domain" nomenclature of NRPSs); TCA, trichloroacetic acid; TLC, thin-layer chromatography.

10.1021/bi011595t CCC: $20.00
Published on Web 11/29/2001

and an amino acid selective nucleophilic acceptor site. Recently, the amino acid selective acceptor site was found to be responsible for preventing internal mis-initiation and to control the timing of substrate epimerization in NRPSs (*15*). The PCP bound aminoacyl substrate is trapped in the nucleophilic acceptor site of the C domain until the peptide bond with the incoming aminoacyl (or peptidyl) chain attached to the electrophilic donor site of the same C domain has been formed. The peptide intermediate is then optionally epimerized in the presence of an epimerization domain and subsequently transferred to a downstream module, and the reaction cycle is repeated.

In nature, two alternative ways of D-amino acid incorporation in NRPSs products are realized. In some cases, an external racemase generates the desired D-amino acids, which are subsequently recognized and selectively activated by the A domain. Most common, however, L-amino acids are activated by modules that comprise an epimerization (E) domain that is responsible for the conversion to the D-isomer. They represent a class of cofactor independent amino acid epimerases that catalyze the de- and reprotonation of the α-carbon atom of an enzyme bound aminoacyl- or peptidyl-S-Ppant in both directions (L-to-D and D-to-L), resulting in a mixture of both isomers (*16*, *17*). However, the L-aminoacyl- or peptidyl-S-Ppant is discriminated by the enantioselectivity of the donor site of the following C domain, leading to a single product with D-configuration. Recently, mutational analysis of 22 conserved residues within an E domain was reported. However, little was revealed about the mechanism of this reaction (*17*).

The D-amino acids are very important for the pharmacological activity of NRPSs products. Furthermore, the corresponding E domains are very often found at the C-terminal ends of bacterial NRPSs and are supposed to be involved in the correct recognition of downstream synthetases (*13*, *17*). This makes them a potential target for future combinatorial approaches.

To investigate the specificity and portability of E domains, being important for the suitability of the E domains in such engineering approaches, a set of eight fusion proteins (see Figure 2B) of the type A/PCP-E and A-PCP/E (in Figure 1, the reactions catalyzed by such A-PCP-E modules are shown) was constructed and tested for epimerization activities. We were able to show that an E domain is functionally portable to other A domains and capable of epimerizing altered substrates (Trp, Val, and Ile instead of Phe). Epimerization activity relies, however, on the presence of a designated PCP domain.

EXPERIMENTAL PROCEDURES

Cloning of the Recombinant Peptide Synthetase Genes and Protein Overproduction. All plasmids used are based on the pQE vector system from Qiagen (Qiagen, Hilden, Germany). Standard procedures were applied for PCR amplification, purification, and cloning of recombinant DNA (*18*). For cloning, *Escherichia coli* XL1 Blue (Stratagene, Heidelberg, Germany) was used.

The primers used in this study are summarized in Table 1 (numbered from P1 to P35); the fragments amplified for the construction of the gene fragments encoding the set of the eight fusion proteins are presented in Figure 2A. The

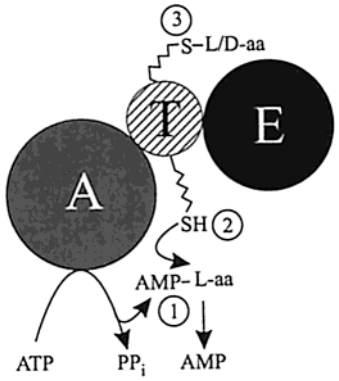

FIGURE 1: Reactions catalyzed by an ATE module. (1) The A domain recognizes the substrate amino acid. Under consumption of ATP, aminoacyl-O-AMP and inorganic PP_i are formed. (2) The aminoacyl-O-AMP is subsequently transferred to the cofactor 4′-phosphopantetheine, which has been covalently tethered to an invariant serine residue of the paired PCP (T domain) by a dedicated 4′-phosphopantetheinyltransferase. Under release of AMP, aminoacyl-S-Ppant is formed. (3) The aminoacyl-S-Ppant is subsequently epimerized by the E domain, and a mixture of L- and D-isomers is formed. The following C domain discriminates against the L-isomer, and only the D-isomer is incorporated into the peptide product synthesized.

fragments based on the genes encoding the tyrocidine synthetases (*19*) were obtained by PCR amplification with chromosomal DNA of *Bacillus brevis* ATCC 8185 as the template (for the sequence of the oligonucleotides, see Table 1): tycA-TE P1 and P2; tycA-E P3 and P2; $tycB_2$-A P4 and P5; $tycB_2$-AT P6 and P7; $tycB_3$-A P8 and P9; $tycB_3$-AT P8 and P10; $tycC_4$-A P11 and P12; $tycC_4$-AT P11 and P13; tycA-AT P14 and P15; $tycB_3$-E P16 and P17. The cloning procedures for the gene fragments encoding TycA (*20*), $TycB_1$-CAT (ProCAT) (*20*), $TycB_3$-ATE (*15*), and GrsA (*13*) were described previously. The gene fragment *grsA-E* (*Bacillus brevis* ATCC 9999), encoding the E domain of GrsA (*21*), was amplified using the primers P18 and P19. The $bacA_1$-A gene fragment of the bacitracin operon (*22*) was amplified using chromosomal DNA of *Bacillus licheniformis* strain ATCC 10716 with primers P20 and P21.

After cloning these PCR fragments (1, 2, 4, 5, 6, 7, 8, and 10; see Figure 2), except $tycB_2$-A (3), $bacA_1$-A (9), and grsA-E (1′), in pQE vectors, the vectors containing the E domain fragments were digested with a restriction endonuclease cutting directly at the 5′-prime end of the insert (see primer sequences for recognition sites) and a second restriction endonuclease cutting within the vector (*Nde*I or alternatively *Xba*I). Plasmids, containing the A domain coding fragments, were digested with a restriction endonuclease directly cutting at the 3′-end (see primer sequences for recognition sites) of the insert and a second one cutting in the vector being compatible to the corresponding E domain fragments. After DNA purification, the compatible fragments were ligated yielding the vectors carrying the gene fragments for the desired fusion proteins. The plasmids carrying the genes encoding for the hybrid proteins $TycB_2$-A/TE (Ia) and $BacA_1$-A/TE (IVa) were obtained by ligating the *Pst*I/*Nco*I digested PCR fragments of the A domains ($tycB_2$-A and $bacA_1$-A) directly to a pQE vector derivative digested with the same enzymes. This vector derivative contained the TycA-PCP-E gene and was amplified before using the pQE60-tycA vector (*20*) as a template with the primers P22

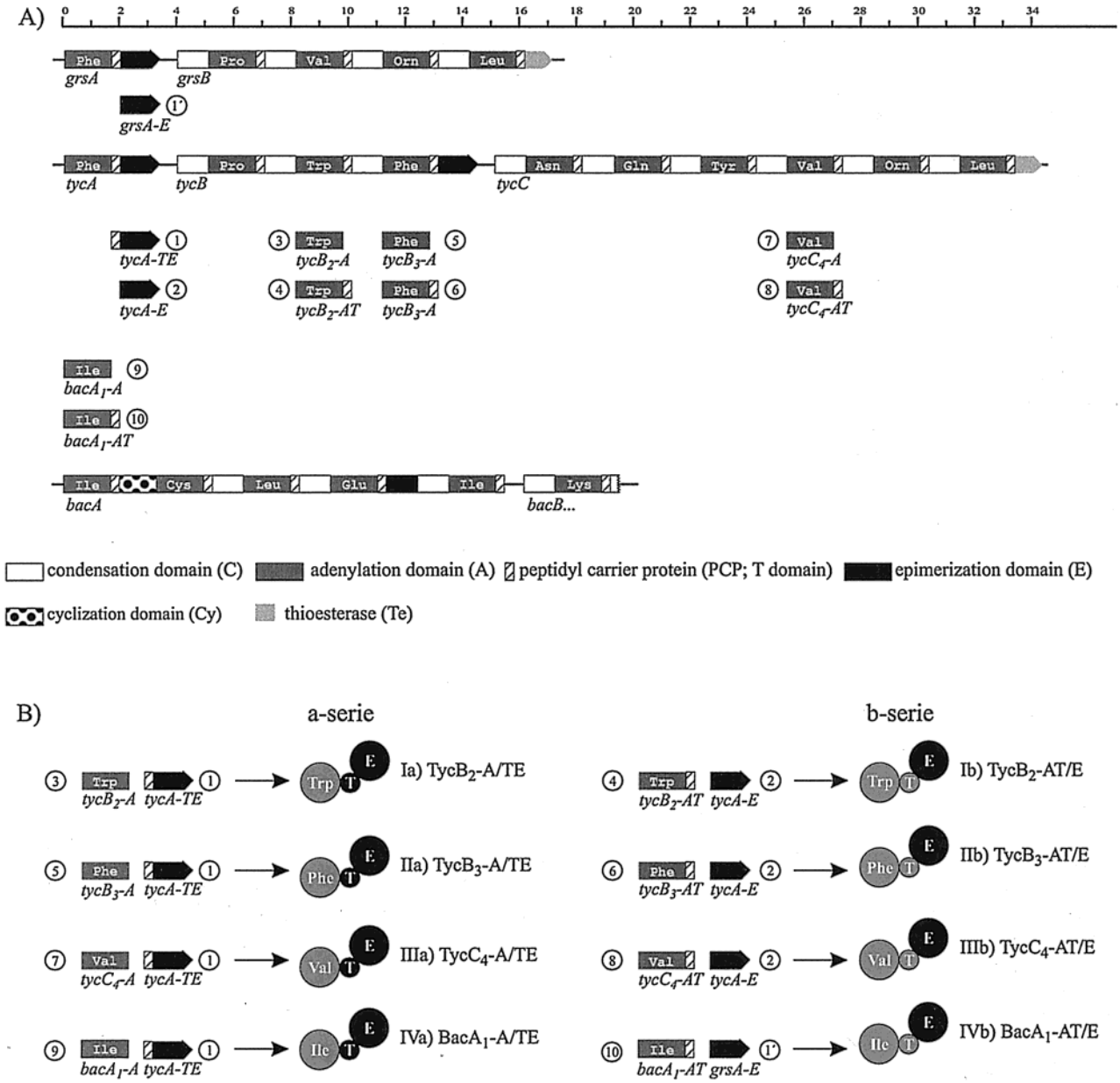

FIGURE 2: (A) Schematic representation of the biosynthesis operons of gramicidin (*Bacillus brevis* ATCC9999), tyrocidine (*Bacillus brevis* ATCC8185), and the first part of the bacitracin operon (*Bacillus licheniformis* ATCC10716). The gene fragments amplified for the construction of the fusion proteins shown in (B) are presented considering their relative locations in the operons. They are numbered from 1 to 10. (B) The combination strategy of the gene fragments presented in (A) is shown. In the a-series, gene fragments encoding an A domain were combined with the fragments encoding PCP-E domains of TycA resulting in constructs for the expression of four fusion proteins of the type A/TE: $TycB_2$-A/TE (Ia), $TycB_3$-A/TE (IIa), $TycC_4$-A/TE (IIIa), and $BacA_1$-A/TE (IVa). In the b-series, the gene fragments encoding A-PCP domains were combined with an E domain, resulting in constructs for the expression of four fusion proteins of the type AT/E: $TycB_2$-AT/E (Ib), $TycB_3$-AT/E (IIb), $TycC_4$-AT/E (IIIb), and $BacA_1$-AT/E (IVb). The fusion site is indicated by light and dark gray coding of the domains.

and P23. The vector, containing the $bacA_1$-AT-grsA-E gene, was constructed by a similar procedure. Digested grsA-E (*Spe*I, *Bam*HI) was ligated in a digested pQE-$bacA_1$-AT vector derivative (*Spe*I, *Bgl*II) obtained by PCR amplification with pQE-$bacA_{1-2}$-AT.CyAT as the template and the P24 and P25. The plasmid pQE-$bacA_{1-2}$-AT.CyAT was derived by amplification of the $bacA_{1-2}$-AT.CyAT gene fragment using chromosomal DNA of *Bacillus licheniformis* strain ATCC 10716 with the primers P26 and P27 and subsequent cloning into a pQE60 vector.

The plasmids encoding the GrsA mutants were generated by utilizing the Quick Change Site Directed Mutagenesis Kit (Stratagene, Heidelberg, Germany) as described by manufacturers' protocols. A pQE60 plasmid (Qiagen, Hilden, Germany) carrying the DNA encoding GrsA was used (*13*) with the following primers: grsA-ASI P28 and P29; grsA-HSI P30 and P31; grsA-HSL P32 and P33; grsA-DSL P34 and P35.

E. coli M15/pREP4 was transformed separately with all plasmids described. Expression and purification of the His_6-tagged apo-proteins were performed as previously described (*13*). Overproduction and purification after single-step Ni^{2+}-affinity chromatography were confirmed by SDS-PAGE (*23*). The protein concentrations were assigned using the method

Table 1: Oligonucleotides Used in This Study[a]

no.	oligonucleotide sequence
P1	5′-TAA**AGATCT**GCCTACCATCCTCCG-3′
P2	5′-TAT**GGATCC**GCGCAGTGTATTTGCAAG-3′
P3	5-ATA**AGATCT**AGAAAAAGCGATCAGGGCATC-3′
P4	5′-CAA**CCATGG**AGATGCTGACTGCGCATG-3′
P5	5′-AGC**CTGCAG**TGTTGCAGGCTTTCCTTCC-3′
P6	5′-AAT**GCATGC**TGACTGCGCATGAG-3′
P7	5′-ATA**GGATCC**TTCGATCAAGCGGGCCAAGTC-3′
P8	5′-AAA**GCATGC**TGACAGCAGCAG-3′
P9	5′-AAA**GGATCC**CCGGTTCTCCTCCTGGTTC-3′
P10	5′-AAA**GGATCC**CGGGATGACGCGCAGAG-3′
P11	5′-AAT**CCATGG**TCAGCGAGGAAGAGCG-3′
P12	5′-AAA**GGATCC**TGTCGTCCGCTCG-3′
P13	5′-AAA**GGATCC**GGCAATATGCGCAGCCAAC-3′
P14	5′-ATA**CCATGG**TAGCAAATCAGGCCAATC-3′
P15	5′- AAA**GGATCC**GCTTTGGTTTGCCGTAAG-3′
P16	5′- AAA**AGATCT**CGAGAGAGCGAGCAGG-3′
P17	5′-ATA**GGATCC**AATCCATTCCAGGATGTTTTCC-3′
P18	5′-TTT**ACTAGT**AAAAGAAGAAGTGAGCAAGG-3′
P19	5′-ATA**GGATCC**CGTTAATGAATCGGCCAAC-3′
P20	5′-TTT**CCATGG**CTAAACATTCATTAGA-3′
P21	5′-TTC**CTGCAG**CGCCCCCGCCGTTCTG-3′
P22	5′-AGC**CTGCAG**GCCTACCATCCTCCGAG-3′
P23	5′-TGGAC**CCATGG**TAATTTCTCCTCT-3′
P24	5′-TTT**ACTAGT**AAAAGAAGAAGTGAGCAAGG-3′
P25	5′- GGAAGCGATATGGAACATCC-3′
P26	5′-TATA**CCATGG**TTGCTAAACATTCATT-3′
P27	5′-TAAC**AGATCT**TTGTTGGGCAGGG-3′
P28	5′-CTATGCATTAGGTGGAGCTTCTATTAAAGCAATACAGGTTGCTGC-3′
P29	5′-GCAGCAACCTGTATTGCTTTAATAGAAGCTCCACCTAATGCATAG-3′
P30	5′-CTATGCATTAGGTGGACATTCTATTAAAGCAATACAGGTTGCTGC-3′
P31	5′-GCAGCAACCTGTATTGCTTTAATAGAATGTCCACCTAATGCATAG-3′
P32	5′-CTATGCATTAGGTGGACATTCTCTTAAAGCAATACAGGTTGCTGC-3′
P33	5′-GCAGCAACCTGTATTGCTTTAAGAGAATGTCCACCTAATGCATAG-3′
P34	5′-CTATGCATTAGGTGGAGATTCTCTTAAAGCAATACAGGTTGCTGC-3′
P35	5′-GCAGCAACCTGTATTGCTTTAAGAGAATCTCCACCTAATGCATAG-3′

[a] Restriction sites are highlighted by bold letters, while mutations introduced in *grsA* (primers P28-35) are underlined.

of Bradford (*24*). After dialysis against assay buffer (50 mM HEPES (pH 8.0), 200 mM NaCl, 1 mM EDTA, 2 mM DTE, 10 mM $MgCl_2$), the proteins were shock-frozen in liquid nitrogen and could be stored at −80 °C over several weeks without significant loss of activity.

Sequence Alignments of PCP Domains. The sequences of PCP domains were retrieved from publicly accessible databases (NCBI, Swiss-Prot, etc.). The sequences used were derived from biosynthesis operons of gramicidin S (Grs), tyrocidine (Tyc), and bacitracin (Bac). After outlining the 80 aa (PCP^E) and 81 aa (PCP^C) stretches, the sequences were aligned.

Posttranslational Modification of the Enzymes by Sfp and CoASH. Priming of heterologously expressed proteins was carried out in vitro by addition of 200 μM CoASH and 15 nM recombinant *Bacillus subtilis* Ppant-transferase *Sfp* (*12*) to all assays which needed holo-enzymes. After preincubation of the samples for 10 min at 37 °C, the assays were started by addition of the amino acids.

ATP−PP_i Exchange Reaction. The A domain activity, specificity, and correct folding of all fusion proteins constructed were examined by applying the ATP−PP_i exchange assay (*15*). We tested the cognate substrate amino acids relevant for the subsequent epimerization assays.

Aminoacylation Assay. To a reaction mixture containing 500 nM enzyme, 50 mM HEPES (pH 8.0), 200 mM NaCl, 1 mM EDTA, 10 mM $MgCl_2$, and 1mM ATP being equilibrated (10 min) to a temperature of 37 °C were rapidly added [^{14}C]-labeled substrate amino acids to a final concentration of 2.5 μM. At various time points, 200 μL aliquots were taken and immediately quenched by addition of 1 mL of ice-cold TCA (10%). After 15 min of incubation on ice, samples were centrifuged (4 °C, 13 000 rpm) for 20 min, washed twice with 1 mL of ice-cold TCA, redissolved in 150 μL of formic acid, and quantified by LSC. The highest value obtained by LSC was specified as 100% aminoacylation, and all other values were calculated relative to this value.

DKP Formation Assay. For comparison of DKP production rates (13), GrsA and the GrsA mutants (ASI, HSI, HSL, and DSL) (50 nM each) were assayed at 37 °C with 1.25 μM ProCAT, 2.5 mM L- or D-Phe, and 2.5 mM L-Pro for up to 2 h in a final volume of 200 μL. For all enzymes used, the concentrations were normalized for aminoacylation activity, because only the enzymes becoming aminoacylated are in principle able of product formation. Aminoacylation activity was calculated by quantification of enzyme bound radioactivity in the aminoacylation assay. The reaction was stopped by the addition of 1 mL of methanol. After centrifugation (13 000 rpm, 15 min) and transferring the supernatant to a fresh tube, the solvent was removed under vacuum, and the residue was dissolved in 100 μL of 30% methanol (v/v) and applied (25 μL) to HPLC. Separation of the reaction products was achieved on a 70/4 Nucleosil 100-5 C18 reversed phase column (Machery and Nagel, Germany) by applying an isocratic method at a flow rate of 0.6 mL

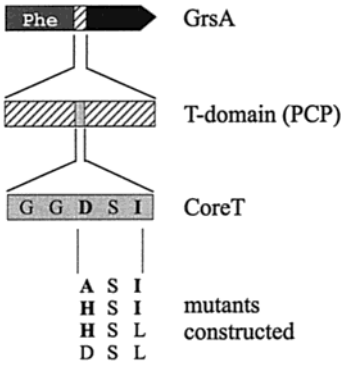

FIGURE 3: The initiation synthetase of gramicidin biosynthesis (*Bacillus brevis* ATCC 9999) is shown in a schematic presentation. The T domain (PCP) and therein the CoreT sequence are enlarged. Wild-type GrsA shows the CoreT signature sequence [GG**D**S**I**]. The CoreT mutations constructed are highlighted by bold letters (GrsA-**A**SI, GrsA-**H**SI, GrsA-**HSL**, and GrsA-DS**L**).

min^{-1} with 30% buffer B (buffer A, 0.05% formic acid/water (v/v); buffer B, 0.045% formic acid/methanol (v/v)). The amount of product formed was determined by detector calibration with different amounts of standard.

Radio-TLC Assay for Detection of Aminoacyl-S-Ppant Epimerization. To monitor the epimerization activity of all fusion proteins and GrsA mutants constructed, the enzymes were allowed to activate and covalently load the cognate [^{14}C]-amino acids. The assay conditions used were as previously described (*15*).

RESULTS

Generation and Purification of the Recombinant Enzymes. In this study, we designed a set of eight recombinant fusion proteins, in which we have fused an epimerization domain with several adenylation domains (see Figure 2A). All fusions were done at DNA level. The E or the PCP-E domains of $TycA_{(Phe)}$ were combined with the A or A-PCP domains of $TycB_{2(Trp/Phe)}$, $TycB_{3(Phe)}$, $TycC_{4(Val)}$, and $BacA_{1(Ile)}$ resulting in hybrid A-PCP-E modules (reactions catalyzed by A-PCP-E modules are presented in Figure 1): $TycB_2$-A/TE (Ia), $TycB_2$-AT/E (Ib), $TycB_3$-A/TE (IIa), $TycB_3$-AT/E (IIb), $TycC_4$-A/TE (IIIa), $TycC_4$-AT/E (IIIb), $BacA_1$-A/TE (IVa), and $BacA_1$-AT/E (IVb) (see Figure 2B). The latter one harbors the E domain of gramicidin S synthetase GrsA, which is very similar to TycA-E. Further, the E domain of $TycB_{3(Phe)}$ was directly fused at DNA level to the A-PCP domains of $TycA_{(Phe)}$ encoding the enzyme TycA-AT-$TycB_3$-E.

Additionally, four PCP CoreT mutants of GrsA were generated by introducing the following point mutations into wild-type GrsA (see Figure 2): the single mutants GrsA-ASI, GrsA-HSI, and GrsA-DSL, as well as the double mutant GrsA-HSL (in brackets, the last three amino acids of CoreT (GG[H,D]S[L,I]) are shown; mutations are highlighted by underlined letters). In the latter construct, the CoreT motif resembles the Ppant binding motif of ordinary C-A-PCP elongation modules (rather than epimerizing C-A-PCP-E modules). The integrity of all constructs (especially the sequences of the regions encoding PCP and E domain) was verified by DNA sequencing (Figure 3).

All proteins were individually expressed as C-terminal His_6-tag fusions in the heterologous host *E. coli* and could be purified to homogeneity by Ni^{2+} affinity chromatography (confirmed by SDS-PAGE, data not shown). Proteins $TycB_2$-A-TycA-TE (Ia) and $TycB_3$-A-TycA-TE (IIa) showed a 10-fold reduced thiolation activity. However, this problem could be solved by altering the expression conditions (22 °C, overnight).

Table 2: Half-Times of Aminoacylation Reaction

	A/TE	AT/E
$TycB_2$-	240 s	<15 s
$TycB_3$-	75 s	40 s
$TycC_4$-	150 s	40 s
$BacA_1$-	20 s	<15 s

Amino Acid Activation (PP_i Exchange Assay). The A domains of GrsA, $TycB_2$, and $TycB_3$ have been described as Trp and Phe activating domains (*19*), while $TycC_4$-A and $BacA_1$-A activate Val (*19*) and Ile (*22*), respectively. To examine for correct folding of all fusion proteins constructed, an amino acid-dependent ATP−PP_i exchange assay was carried out. All recombinant enzymes were found to activate their cognate amino acids, indicating their correct folding (data not shown). Obviously, the A domains' selectivity was not significantly affected by the domain fusions conducted.

Investigating Aminoacylation Efficiency. It is known that different modules of NRPSs show differences in their aminoacylation kinetics, but little was known about the influence of a domain fusion between A and PCP domains on this reaction. By comparing the time dependence of the aminoacylation reactions for A/PCP-E and A-PCP/E fusions (see Figure 4), we were able to get some interesting information on the influence of A and PCP domain−domain interaction on aminoacylation efficiency. After the addition of radiolabeled substrate amino acid to the reaction mixture, samples were taken at defined time points and immediately quenched by the addition of 10% TCA. Subsequently, the amount of acid-stable label was determined by LSC. The highest value obtained was defined to 100% aminoacylation, and all other values calculated as relative amounts were compared to the maximum.

The results of these experiments are summarized in Figure 4 and Table 2. All reactions were performed at least in triplicate, and the estimated margin of error was approximately ±4%. $TycB_2$-AT/E (Ib) shows about 100% aminoacylation at all time points measured when incubated with Trp as a substrate amino acid (Figure 4a). For the corresponding enzyme $TycB_2$-A/TE (Ia), it takes about 4 min to achieve 50% aminoacylation, indicating a disturbed communication between A and PCP. $TycB_3$-A/TE (IIa) and $TycB_3$-AT/E (IIb) show similar aminoacylation properties when L-Phe is used as the substrate, although the latter one seems to be slightly (2 times) faster (see Figure 4b). $TycC_4$-AT/E (IIIb) is significantly faster (4 times) than $TycC_4$-A/TE (IIIa), while $BacA_1$-A/TE (IVa) and $BacA_1$-AT/E (IVb) show only little differences in aminoacylation kinetics (see Figure 4c and d). Summarizing the results, it is obvious that the A/PCP-E fusion proteins (Ia, IIa, IIIa, and IVa) are at least somewhat impaired in their respective aminoacylation activity when compared to the corresponding enzymes, featuring an A-PCP/E-type of fusion (Ib, IIb, IIIb, and IVb). This indicates that during evolution at least some optimiza-

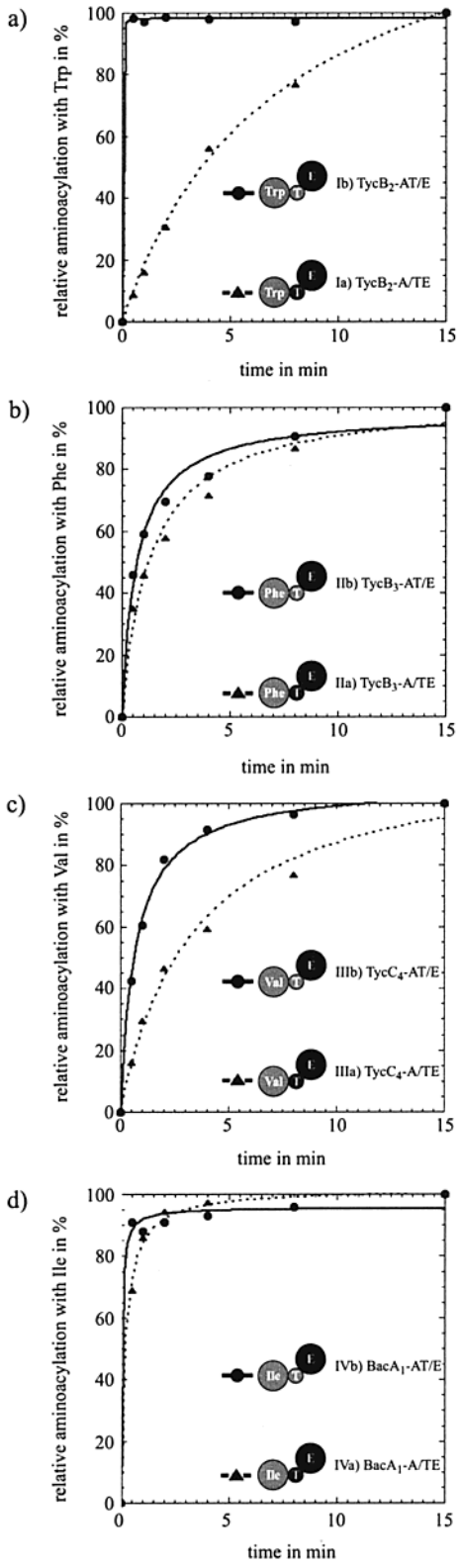

FIGURE 4: Aminoacylation kinetics of the fusion proteins (a) $TycB_2$-A/TE (Ia) and $TycB_2$-AT/E (Ib), (b) $TycB_3$-A/TE (IIa) and $TycB_3$-AT/E (IIb), (c) $TycC_4$-A/TE (IIIa) and $TycC_4$-AT/E (IIIb), and (d) $BacA_1$-A/TE (IVa) and $BacA_1$-AT/E (IVb). The holo-enzymes were rapidly mixed with a 5-fold excess of [^{14}C]-labeled substrate amino acids. At defined time points, aliquots were taken, and the reaction was quenched immediately by the addition of 10% TCA. The highest amount of acid stable label was specified to 100% aminoacylation. All other values are shown as relative values in percent of the maximum: triangles, fusion proteins of the type A/PCP-E (A/TE; Figure 2, a-series); circles, fusion proteins of the type A-PCP/E (AT/E; Figure 2, b-series).

tion for the interaction between A domain and the partner PCP took place. Despite these differences, all fusion proteins (A/PCP-E and A-PCP/E) revealed a sufficient aminoacylation, allowing the further investigation of their epimerization activities.

Epimerization Activity of the Fusion Proteins. Epimerization domains catalyze the L-to-D and D-to-L conversion of aminoacyl-S-Ppant or peptidyl-S-Ppant substrates. In the case of GrsA, it was shown that substrate epimerization is exceedingly fast (milliseconds) in reaching a 2:1 equilibrium of D-/L-aminoacyl-S-Ppant enzyme (*17*, *25*).

The extent of aminoacyl-S-Ppant epimerization was investigated by the dependence of time with L-[^{14}C]-labeled substrate amino acids for all fusion proteins. Apparent k_{cat} values were calculated out of these data except in the case of the fast reactions finished at the earliest time point assessed by our assay (30 s). There rapid quench studies are recommended to calculate these values. All reactions were carried out in triplicate. The margin of error was estimated to be approximately $\pm$5%.

The results of the epimerization assays of the eight fusion proteins are shown in Figure 5. The A domain of $TycB_2$, utilized in the hybrid proteins $TycB_2$-A/TE (Ia) and $TycB_2$-AT/E (Ib), was previously described as a Trp activating domain (*19*, *26*), but the use of Phe as a substrate amino acid was also possible and led to comparable results (data not shown). In the case of $TycB_2$, $TycC_4$, and $BacA_1$ fusions, only the A/PCP-E type of fusion showed epimerization activity (Ia, IIIa, and IVa), while both $TycB_3$-A/TE and $TycB_3$-AT/E (IIa and IIb) were capable of epimerizing L-Phe-S-Ppant (Figure 5b). In contrast to the other non-epimerizing fusion proteins of the type A-PCP/E, $TycB_3$-AT/E (IIa) is the only one containing a PCP^E of $TycB_3$. $TycB_2$-A/TE (Ia) ($\sim$54% D-Trp-S-Ppant), $TycB_3$-A/TE (IIa) ($\sim$57% D-Phe-S-Ppant), $TycC_4$-A/TE (IIIa) ($\sim$64% D-Val-S-Ppant), and $BacA_1$-A/TE (IVa) ($\sim$60% D-allo-Ile-S-Ppant), all carrying the PCP^E of TycA, reached similar equilibrium positions, while $TycB_3$-AT/E (IIb), carrying the PCP^E of $TycB_3$, revealed a different equilibrium position at $\sim$43% D-Phe-S-Ppant. While the latter one reached this equilibrium position in less than 30 s (earliest time point measured, k_{cat} not determined), $TycB_2$-A/TE (Ia) (k_{cat} 6.7 min^{-1}), $TycB_3$-A/TE (IIa) (k_{cat} 7.3 min^{-1}), and $TycC_4$-A/TE (IIIa) (k_{cat} 1.7 min^{-1}) were marginally slower. $BacA_1$-A/TE (IVa) (k_{cat} 0.3 min^{-1}), in contrast, was significantly slower.

The comparison of the time courses of substrate epimerization for the wild-type A-PCP-E modules TycA and $TycB_3$ is also very interesting, as well as the fusion proteins TycA-AT-$TycB_3$-E and $TycB_3$-A/TE (IIb) (Figure 6). These constructs feature an E domain normally epimerizing either an aminoacyl-S-Ppant (TycA and $TycB_3$-A/TE (IIb)) or an peptidyl-S$-$Ppant ($TycB_3$ and TycA-AT/E) substrate. As shown, wild-type TycA is an exceedingly fast aminoacyl-S-Ppant epimerase, having reached the equilibrium between L- and D-Phe-S-Ppant (about 70% D-Phe-S-Ppant) at the earliest time point taken (k_{cat} not determined). The peptidyl-S-Ppant epimerase $TycB_3$, in contrast, is capable of epimerizing an aminoacyl-S-Ppant substrate, although at a significantly lowered rate (k_{cat} 0.2 min^{-1}) (*15*). This reduction in epimerization rate acceleration could be overcome by replacing the peptidyl-S-Ppant specific E domain of $TycB_3$ against the aminoacyl-S-Ppant specific E domain of TycA (resulting

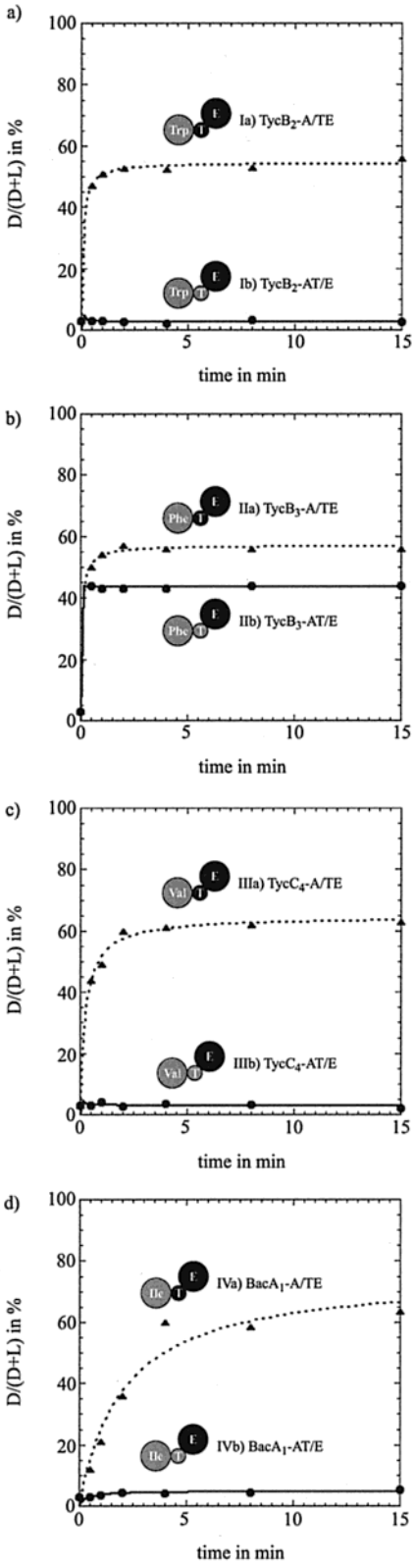

FIGURE 5: L-to-D conversion in the amino acid-S-Ppant complexes of the fusion proteins (a) $TycB_2$-A/TE (Ia) and $TycB_2$-AT/E (Ib), (b) $TycB_3$-A/TE (IIa) and $TycB_3$-AT/E (IIb), (c) $TycC_4$-A/TE (IIIa) and $TycC_4$-AT/E (IIIb), and (d) $BacA_1$-A/TE (IVa) and $BacA_1$-AT/E (IVb). The amount of [^{14}C]-labeled D-amino acid found after TCA-precipitation and thioester cleavage of the amino acid-S-Ppant-enzyme complexes is shown in percent of total amount of radioactivity in the dependence of time: triangles, fusion proteins of the type A/TE (a-series); circles, fusion proteins of the type AT/E (b-series). The data for wild-type TycA are presented in the same way in Figure 6.

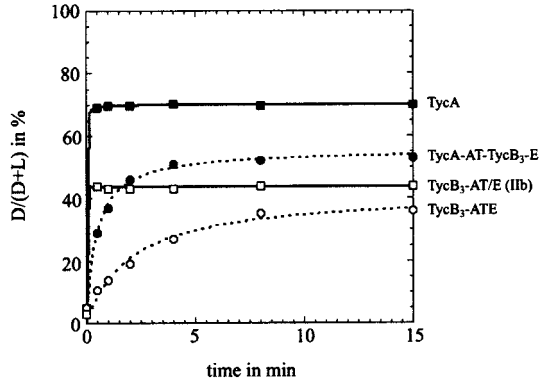

FIGURE 6: Comparison of the L-to-D conversion in the Phe-S-Ppant complexes of the proteins TycA, TycA-AT-$TycB_3$-E, $TycB_3$-ATE, and $TycB_3$-AT/E. Open symbols represent enzymes with the PCP of $TycB_3$, and closed symbols represent enzymes with the PCP (T domain) of TycA. Proteins harboring the E domain of TycA are symbolized by a straight line, while those with the E domain of $TycB_3$ are symbolized by a dotted line. Squares indicate a wild-type enzyme, while circles represent a fusion protein. The amount of [^{14}C]-labeled D-amino acid found after TCA-precipitation and thioester cleavage of the amino acid-S-Ppant-enzyme complexes is shown in percent of total amount of radioactivity in the dependence of time.

construct: $TycB_3$-A/TE (IIb) (k_{cat} 7.3 min^{-1})). The exact opposite holds true for the substitution against a peptidyl-S-Ppant specific E domain, as realized in our construct TycA-AT/$TycB_3$-E (k_{cat} 0.8 min^{-1}). Here, the epimerization rate sustained a significant drop. Notably, in this latter construct, equilibration between D- and L-Phe-S-Ppant takes place considerably faster (4 times) than it does in the case for the wild-type A-PCP-E construct $TycB_3$, indicating that also the PCP domain might contribute to the epimerization activity in corresponding NRPS modules. In the fusion protein tested, the nature of the PCP domain may also influence the equilibrium position between the D- and L-isomer, since constructs featuring the PCP domain of TycA revealed a considerably higher share on D-Phe-S-Ppant (about 55−70%) than on those proteins carrying the PCP of $TycB_3$ (only approximately 40%).

Sequence Alignments of Different PCPs. Recently, a phylogenetic study revealed a clustering of PCPs in NRPS according to the partner domains they are connected to (C versus E domain) (*27*). However, no specific conserved sequence variations were reported for both types of PCPs. The biochemical data obtained in our study indicated that there are obviously functional differences between different types of PCPs, which should be reflected in varying primary sequences. The fusion proteins carrying PCP^Cs, for example, showed no E domain activity (Ib, IIIb, and IVb), while those harboring a PCP^E ($TycB_3$-AT/E (IIb)) did.

Therefore, we aligned several PCP domains to reveal if differences on the primary sequence exist. The results are shown in Figure 7. The major differences of PCP^Es as compared to PCP^Cs are (i) the signature core T motif (GGDSI) (in contrast to (GGHSL)), (ii) a highly conserved Gln residue in position 50 (numbering according to the NMR structure of $TycC_3$-PCP published (*10*)), (iii) a deletion of one amino acid in position 58, (iv) no conserved Pro and Glu residues in positions 64 and 70, respectively, and (v) an acidic residue in position 67 (Asp or Glu) instead of a hydrophobic residue. Interestingly, all sequence variations

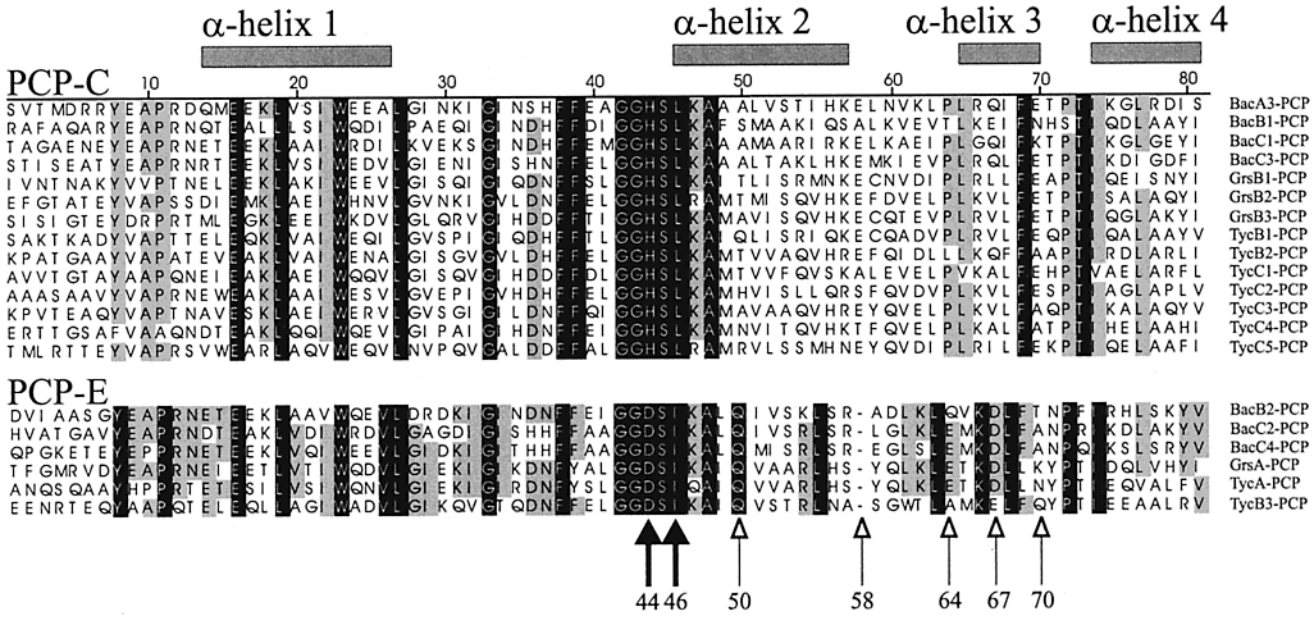

FIGURE 7: Comparison of sequence alignments of PCP^{C}s to PCP^{E}s. Sequences used were derived from the biosynthesis operons of bacitracin, gramicidin S, and tyrocidine. The gray bars on the top of the figure demonstrate the positions of the four α-helices found in the structure of $TycC_3$-PCP (*10*). Numbering is done according to this published structure. The bold arrows indicate the two positions being different in CoreT of the two types of PCPs, while the bright arrows show additional differences found within the α-helices 2 and 3.

observed are localized within the α-helices 2 and 3 of PCPs, being at the same face of the reported NMR structure (*10*).

Epimerization Activity of the GrsA Mutants. As presented up to here, NRPS assembly lines feature two types of PCP domains, which can be distinguished on account of their respective primary sequences and their capability to interact with certain tailoring domains (i.e., E domain). The most obvious structural difference concerns the highly conserved Ppant binding motif CoreT, where two amino acid substitutions (H44D and L46I) could be observed (Figure 7). To find out whether these variations are important for an efficient interaction with a preceding E domain, a set of four PCP domain mutants was constructed in the TycA-homologue GrsA (GrsA-ASI, GrsA-HSI, GrsA-HSL, and GrsA-DSL; see Figure 2). After purification and basic biochemical characterization, the mutants were allowed to activate and load either L- or D-[^{14}C]-Phe. The resulting [^{14}C]-Phe-S-Ppant-enzyme complexes were separated from excess substrate, washed, and hydrolyzed with 0.1 M potassium hydroxide. The released [^{14}C]-Phe could then be applied to chiral TLC plates to determine the stereochemistry of the released amino acid.

The results of the epimerization assays of the GrsA CoreT mutants are summarized in Figure 8. GrsA is a very efficient enzyme, and the equilibrium position of about 63% D-Phe-S-Ppant is reached within milliseconds (*25*). According to our epimerization assay conducted, mutants GrsA-ASI (k_{cat} not determined) and GrsA-DSI (k_{cat} not determined) behaved like wild-type GrsA, although it has to be noted that the earliest time point taken was 30 s after initiation of the reaction. Consequently, we cannot exclude that differences to wild-type GrsA could be found if rapid quench kinetics would be applied. The other two mutants, GrsA-HSI (k_{cat} 1.9 min^{-1}) and GrsA-HSL (k_{cat} 0.2 min^{-1}), evidently showed a different behavior, and their equilibrium position was shifted to approximately 80% D-Phe-S-Ppant. Furthermore, the period of time required to reach these equilibria was

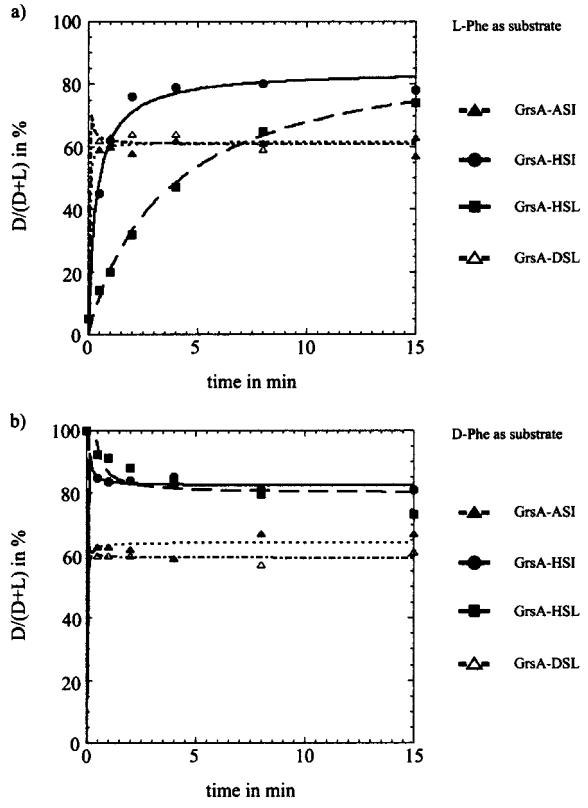

FIGURE 8: (a) L-to-D and (b) D-to-L conversion in the Phe-S-Ppant complexes of the GrsA CoreT mutants GrsA-ASI (triangles, closed symbols), GrsA-HSI (circles), GrsA-HSL (squares), and GrsA-DSL (triangles, open symbols). The data for wild-type GrsA were recently published (*17, 25*). It reaches its equilibrium position (63% D-Phe-S-Ppant) in less than one second.

dramatically increased, when compared to wild-type GrsA (*25*). The double-mutant GrsA-HSL, featuring the CoreT motif of a PCP^{C}, revealed the largest impairment in reaching the equilibrium position, and the k_{cat} was decreased additionally 10-fold as compared to GrsA-HSI.

Table 3: DKP Formation Rates of GrsA and GrsA CoreT Mutants[a]

	K_{obs} in min^{-1} with L-Phe	K_{obs} in min^{-1} with D-Phe
GrsA (wt)	69.6 ± 1.3	65.5 ±0.7
GrsA-ASI	18.5 ± 0.3	61.2 ± 2.7
GrsA-HSI	13.7 ± 0.4	53.7 ± 3.7
GrsA-HSL	16.0 ± 0.4	57.7 ± 4.5
GrsA-DSL	54.4 ± 1.1	65.2 ± 1.7

[a] Rates were determined with a 25-fold excess of $TycB_1$-CAT.

DKP Formation Activity of GrsA CoreT Mutants As Compared to Wild-Type GrsA. GrsA is the initiation synthetase of gramicidin S biosynthesis in *B. brevis*. It was reported that GrsA is able to transfer D-Phe to $TycB_1$-CAT (ProCAT), the first module of tyrocidine synthetase B, in vitro. The linear D-Phe-L-Pro formed is then released from the enzyme as cyclic D-Phe-L-Pro-DKP by a noncatalyzed reaction (*13*). We found GrsA to interact with the $TycB_1$-CAT enzyme in a catalytic but not stoichiometric way, because the total amount of DKP synthesized during the assay was dependent on the $TycB_1$-CAT concentration (data not shown). So obviously, the noncatalyzed DKP release from $TycB_1$-CAT is the rate-limiting step of DKP formation, and the protein−protein interaction of GrsA with $TycB_1$-CAT is not static. Because we wanted to investigate the effect of the mutations in the E domain of GrsA on product formation efficiency, we used $TycB_1$-CAT in a 25-fold excess to be sure that a further increase of $TycB_1$-CAT does not interfere with the amount of DKP formed and, as a consequence of this, that the measured rates of GrsA and GrsA CoreT mutants are not limited by the $TycB_1$-CAT concentrations but by the mutations in the E domain.

The assay was done separately with L-Phe and D-Phe as substrates for GrsA and GrsA CoreT mutants. The results are summarized in Table 3. Interestingly, wild-type GrsA shows a high turnover rate under the reaction conditions used. The k_{obs} is 69.6 ± 1.3 for L-Phe and 65.5 ± 0.7 with D-Phe as the substrate. As expected because of the epimerization assay of GrsA-DSL, no significant loss of activity in the DKP formation assay was observed. The k_{obs} when L-Phe is utilized as substrate is 54.4 ± 1.1; with D-Phe it is 65.2 ± 1.7. All other mutants are impaired in product formation activity when L-Phe is utilized as the substrate (GrsA-ASI 18.5 ± 0.3; GrsA-HSI 13.7 ± 0.4; GrsA-HSL 16.0 ± 0.4), while when using D-Phe as the substrate (similar substrate as L-Phe for activation and aminoacylation), all k_{obs} values are in the same range as determined for wild-type GrsA (GrsA-ASI 61.2 ± 2.7; GrsA-HSI 53.7 ± 3.7; GrsA-HSL 57.7 ± 4.5). The results are summarized in Table 3.

DISCUSSION

Generally, D-amino acids are important for bioactivity of many nonribosomal peptide antibiotics (*4*), and, consequently, E domains play an important role in NRPS assembly lines. These domains, which catalyze the conversion of L- into D-amino acids, are often found at the C-terminal end of bacterial NRPSs and are therefore involved in the protein−protein interaction between NRPSs (*13*, *17*). In vitro studies revealed that E domains equilibrate the L- and D-isomer of a certain aminoacyl- or peptidyl-S-Ppant substrate (*17*). In the case of the initiation module GrsA of the gramicidin S biosynthetic system, to set an example, it takes less than a second to equilibrate the activated L- or D-Phe-S-Ppant to a final ratio of 2:1 in favor of the D-isomer (*25*). In the course of subsequent peptide bond formation, the downstream C domain discriminates against the L-amino acid, and only the D-isomer gets incorporated into the dipeptidyl-S-Ppant intermediate (*14*).

Although E domains would be important tools for the construction of large combinatorial libraries of nonribosomal peptide antibiotics and to increase their diversity, little is known about their tolerance toward alternate aminoacyl- or peptidyl-S-Ppant substrates, as well as their portability. Recently, it was reported that GrsA, if misprimed with L-Ala-S-Ppant, can epimerize this noncognate substrate and translocates the resulting D-alanyl moiety to the downstream acceptor module $TycB_1$-CAT (*14*). In this study, we have generated several A-PCP/E and A/PCP-E fusion proteins and showed that the E domain of the homologous initiation module TycA, naturally also epimerizing Phe, is capable of epimerizing several alternative substrates (Trp, Val, and Ile), albeit at reduced rates when compared with the wild-type enzyme TycA. Intriguingly, the same E domain was inactive in the hybrid proteins $TycB_2$-AT/E (Ib), $TycC_4$-AT/E (IIIb), and $BacA_1$-AT/E (IVb), while it was active in $TycB_3$-AT/E (IIb). The difference between these fusion proteins is that the latter harbors a PCP^E domain, whereas the other PCPs naturally interact with C domains.

Previously, a phylogenetic clustering of PCPs connected to the same domains was reported (*27*). On the basis of sequence comparison, we found that both types of PCP domains described in this work (PCP^E versus PCP^C) reveal several signature differences. Most notably, we observed two amino acid substitutions within the highly conserved CoreT motif, the site harboring the invariant serine for cofactor binding (see Figure 7). PCP^Cs reveal the signature sequence [GG*HSL*], whereas the CoreT of PCP^Es is described by the consensus sequence [GG*DSI*]. Furthermore, some additional differences were detected at positions 50, 58, 64, 67, and 70 (see Figure 7). Interestingly, all of these variations structurally cluster within the α-helices 2 and 3, when assigned to the structure of $TycC_1$-PCP (*10*). Apparently, this region may facilitate a key interaction between both the PCP and the E domain.

Recently, Schauwecker et al. reported that the E domain of actinomycin synthetase when used in the fusion protein "AcmTmVe" showed no epimerization activity, although it was intact (*28*). It was speculated that this E domain was inactive in the fusion protein because of its combination with a *N*-methyltransferase (M) domain. We cannot exclude such an incompatibility of E and M domains, but by considering our data, it is more likely that the used PCP is normally connected to a C domain and therefore was inactive when fused to the E domain. This hypothesis is supported by the results of our mutational analysis of the CoreT motif presented in this study, which revealed the general importance and influence of the residue immediately preceding the invariant serine residue (DSI versus HSL) on epimerization efficiency. Both mutants GrsA-HSI and GrsA-HSL were dramatically impaired in epimerization activity (k_{cat} 1.9 and 0.2 min^{-1}, respectively), as well as in DKP formation

assay when provided with L-Phe, while GrsA-ASI was only impaired in DKP formation assay. When provided with D-Phe, all GrsA mutants revealed wild-type rates for the DKP formation, indicating that the interplay between the donor aminoacyl-S-Ppant PCP domain and the C domain is not affected by the CoreT mutations. One has to bear in mind, however, that in the cases of the mutants GrsA-ASI and GrsA-DSL, the epimerization reaction was already completed at the earliest time point assessed by our assay. Consequently, rapid quench studies will be required to determine the exact rates and to learn about possible differences between wild-type and CoreT mutants, but, in summary, it is obvious that Asp44 is more important on epimerization efficiency than is Ile46.

Therefore, the CoreT of PCPs clearly affects the epimerization reaction catalyzed by the downstream-located E domains. The most likely explanation for this effect would be that the proper positioning of the aminoacyl-S-Ppant PCP substrate at the E domain is somehow influenced by the mutations of the Asp in CoreT to Ala or His. Moreover, the hypothesis that PCPs are somehow involved in the epimerization reaction is supported by the finding that $TycB_3$-A/TE (IIa) and $TycB_3$-AT/E (IIb) show different equilibrium positions of 55% and 43% D-Phe-S-Ppant, respectively. For wild-type $TycB_3$-ATE, an equilibrium position of ~40% D-Phe-S-Ppant was recently reported (*15*), very close to that found for the latter fusion protein, $TycB_3$-AT/E (IIb), harboring the same PCP domain. Wild-type TycA equilibrates both isomers, D- and L-Phe-S-Ppant, at a ratio of about 2.3:1, and TycA-AT-$TycB_3$-E and all other fusion proteins containing the PCP of TycA revealed comparable high equilibria of up to 60% D-Phe-S-Ppant. The CoreT mutants GrsA-HSI and GrsA-HSL, finally, showed a shift in equilibrium position to about 80% D-Phe-S-Ppant (wild-type GrsA: 63% D-Phe-S-Ppant) and a significantly impaired rate of substrate epimerization (k_{cat} 1.9 and 0.2 min^{-1}, respectively). In conclusion, it seems that both the PCP and the E domain and not the E domain alone determine the final ratio between the D- and L-isomer, as well as the rates of the epimerization reaction in NRPS assembly lines.

Something similar, although not as crucial, may apply for the interplay between PCP and A domains. We observed that all A/PCP-E types of fusions sustained at least some drop (approximately 2 times up to >20 times) in aminoacylation efficiency, when compared to the corresponding wild-type proteins. Recently, two independent studies used different strategies for the generation of module fusions and the construction of hybrid NRPSs, and the fusion sites were placed based on domain fusions between either the A and the PCP domain (*26*) or the PCP and the C domain (*20*). Considering our findings, one would deem the PCP/C fusion the more favorable approach, since mutations in CoreT motif of GrsA had no negative effect on efficiency of the condensation reaction.

In conclusion, we were able to show that the Phe epimerizing E domain of TycA is capable of epimerizing the alternate substrates Trp, Val, and Ile, although at reduced efficiencies. Therefore, they are more specific for their cognate aminoacyl-S-Ppant derivatives. In addition to the A domain selectivity determining the amino acid sequence of the final products, some C domain selectivity (donor and acceptor site selectivity) (*14*, *15*) toward aminoacyl-S-Ppant derivatives was also reported. Together with reduced E domain activity toward noncognate aminoacyl-S-Ppant substrates shown in this work, the controlled engineering of NRPS assembly lines becomes a real challenge. Nevertheless, by finding the influence of PCPs on the epimerization reaction as well as to a minor extent on the thiolation reaction, we obtained valuable information about the domains' partnership and possible fusion sites for domain or module fusions. Obviously, E domains need a PCP^E domain as a partner for being active and show no activity when combined with a PCP^C domain. By our data of the sequence alignments, we would suggest α-helices 2 and 3 of the PCP^E (see Figure 7) as being very important for the protein−protein interaction between PCPs and E domains. Nevertheless, the interaction of the E and C domains will have to be studied extensively in the future for being able to disrupt regular CAT-CAT-CAT patterns by CAT-CATE-CAT constructs. So far, for controlled engineering of NRPS assembly lines, much is still to be learned about the secrets of these interesting enzymes.

ACKNOWLEDGMENT

We thank Dr. Torsten Stachelhaus for valuable suggestions and discussions, as well as for a critical reading of the manuscript. Lin Müller and Alan Tanović supported this work by doing some cloning and enzyme preparation. Dr. Dirk Konz provided plasmid pQE-$bacA_{1-2}$-AT.CyAT. We thank Inge Schüler for excellent technical assistance.

REFERENCES

1. Aharonowitz, Y., Bergmeyer, J., Cantoral, J. M., Cohen, G., Demain, A. L., Fink, U., Kinghorn, J., Kleinkauf, H., MacCabe, A., Palissa, H., and et al. (1993) *Biotechnology (NY) 11*, 807−10.
2. van Wageningen, A., Kirkpatrick, P., Williams, D., Harris, B., Kershaw, J., Lennard, N., Jones, M., Jones, S., and Solenberg, P. (1998) *Chem. Biol. 5*, 155−162.
3. Schwarzer, D., and Marahiel, M. A. (2001) *Naturwissenschaften 88*, 93−101.
4. Marahiel, M. A., Stachelhaus, T., and Mootz, H. D. (1997) *Chem. Rev. 97*, 2651−2673.
5. Cane, D. E., and Walsh, C. T. (1999) *Chem. Biol. 6*, R319−25.
6. Konz, D., and Marahiel, M. A. (1999) *Chem. Biol. 6*, R39−48.
7. Weber, T., and Marahiel, M. A. (2001) *Structure 9*, R3−R9.
8. Conti, E., Stachelhaus, T., Marahiel, M. A., and Brick, P. (1997) *EMBO J. 16*, 4174−83.
9. Stachelhaus, T., Hüser, A., and Marahiel, M. A. (1996) *Chem. Biol. 3*, 913−921.
10. Weber, T., Baumgartner, R., Renner, C., Marahiel, M. A., and Holak, T. A. (2000) *Struct. Fold Des. 8*, 407−18.
11. Lambalot, R. H., Gehring, A. M., Flugel, R. S., Zuber, P., LaCelle, M., Marahiel, M. A., Reid, R., Khosla, C., and Walsh, C. T. (1996) *Chem. Biol. 3*, 923−36.
12. Reuter, K., Mofid, M. R., Marahiel, M. A., and Ficner, R. (1999) *EMBO J. 18*, 6823−6831.
13. Stachelhaus, T., Mootz, H. D., Bergendahl, V., and Marahiel, M. A. (1998) *J. Biol. Chem. 273*, 22773−81.
14. Belshaw, P. J., Walsh, C. T., and Stachelhaus, T. (1999) *Science 284*, 486−9.
15. Linne, U., and Marahiel, M. A. (2000) *Biochemistry 39*, 10439−47.
16. Stein, T., Kluge, B., Vater, J., Franke, P., Otto, A., and Wittmann-Liebold, B. (1995) *Biochemistry 34*, 4633−42.

17. Stachelhaus, T., and Walsh, C. T. (2000) *Biochemistry 39*, 5775−87.
18. Sambrook, J., Fritsch, E. F., and Maniatis, T. (1989) *Molecular Cloning: A Laboratory Manual*, Cold Spring Harbor Laboratory Press, Cold Spring Harbor, NY.
19. Mootz, H. D., and Marahiel, M. A. (1997) *J. Bacteriol. 179*, 6843−50.
20. Mootz, H. D., Schwarzer, D., and Marahiel, M. A. (2000) *Proc. Natl. Acad. Sci. U.S.A. 97*, 5848−53.
21. Krätzschmar, J., Krause, M., and Marahiel, M. A. (1989) *J. Bacteriol. 171*, 5422−5429.
22. Konz, D., Klens, A., Schorgendorfer, K., and Marahiel, M. A. (1997) *Chem. Biol. 4*, 927−37.
23. Laemmli, U. K. (1970) *Nature 227*, 491−493.
24. Bradford, M. M. (1976) *Anal. Biochem. 72*, 248−254.
25. Luo, L., and Walsh, C. T. (2001) *Biochemistry 40*, 5329−5337.
26. Doekel, S., and Marahiel, M. A. (2000) *Chem. Biol. 7*, 373−84.
27. von Döhren, H., Dieckmann, R., and Pavela-Vrancic, M. (1999) *Chem. Biol. 6*, R273−R279.
28. Schauwecker, F., Pfennig, F., Grammel, N., and Keller, U. (2000) *Chem. Biol. 7*, 287−97.

BI011595T